PERGAMON

Quaternary Science Reviews 22 (2003) 209–223

QSR

Investigation of the relationship between permafrost distribution in NW Europe and extensive winter sea-ice cover in the North Atlantic Ocean during the cold phases of the Last Glaciation

H. Renssen[a,b,*], J. Vandenberghe[b]

[a] *Institut d'Astronomie et de Géophysique G. Lemaître, Université catholique de Louvain, 2 Chemin du Cyclotron, B-1348 Louvain-la-Neuve, Belgium*
[b] *Netherlands Centre for Geo-ecological Research (ICG), Faculty of Earth and Life Sciences, Vrije Universiteit Amsterdam, De Boelelaan 1085, NL-1081 HV Amsterdam, The Netherlands*

Received 17 February 2002; accepted 09 October 2002

Abstract

Atmospheric model simulations with different extents of sea-ice are compared with reconstructed European mean annual temperatures derived from permafrost indicators. Analysis of the results suggest that during cold phases of the Last Glacial, the southern margin of permafrost in western Europe was controlled by the latitude of the winter sea-ice margin in the North Atlantic Ocean. In this case reconstructions of permafrost extent in Europe may be used to constrain past winter sea-ice conditions in the North Atlantic Ocean. Accordingly, extensive North Atlantic sea-ice cover southwards to at least 50°N is inferred during four phases of the Last Glaciation: (1) Early Pleniglacial (74–59 cal kyr BP), (2) the Hasselo Stadial (41.5–40 cal kyr BP), (3) the LGM (23–19 cal kyr BP) and (4) the Younger Dryas (12.7–11.5 cal kyr BP). The extensive sea-ice cover for the phase of maximum cold disagrees with recent studies suggesting a relatively warm North Atlantic during the LGM, while it agrees with the original CLIMAP reconstruction. Moreover, the estimate for the Younger Dryas cooling conflicts with reconstructions based on marine proxy data.

1. Introduction

It is important to have a good understanding of past North Atlantic surface conditions, as they may hold clues to the sensitivity of the global ocean circulation to varying forcing factors. The North Atlantic surface conditions of the Last Glacial are, however, still under debate. For instance, sea-surface temperature (SST) reconstructions based on dinoflagellates (deVernal et al., 2000) suggest that the North Atlantic may have been substantially warmer during the Last Glacial Maximum (LGM, ~23–19 cal kyr BP, all dates are in thousand cal years BP based on Martinson et al., 1987; Kitagawa and van der Plicht, 1998; and Stuiver et al., 1998) than inferred in the original CLIMAP (1981) reconstruction (Pinot et al., 1999). CLIMAP proposed a relatively cold North Atlantic with a winter sea-ice cover extending southwards to 45°N. Likewise, the North Atlantic SSTs for the Younger Dryas cold event (YD) are also disputed. Reconstructions for YD SSTs and sea-ice extent based on foraminifera (Sarnthein et al., 1995) and diatoms (Koç et al., 1993) suggest a relatively warm Atlantic Ocean that is in conflict with a strong weakening of the thermohaline circulation that is often proposed for the YD (e.g., Stocker and Wright, 1996; Manabe and Stouffer, 1997; Renssen, 1997; Broecker, 1998). To improve our understanding of North Atlantic surface conditions during these phases, this paper explores the relation between the Atlantic sea-ice cover and past permafrost conditions in NW Europe. For this purpose we combine climate model simulations and geological data giving information on permafrost distribution.

The distribution of permafrost in Europe during various stages of the Last Glacial is relatively well known, as some relic features associated with permafrost are well preserved. Reconstructions of permafrost distribution in NW Europe exist for the following cold

*Corresponding author. Tel.: +31-20-444-7376; fax: +31-20-646-2457.
E-mail address: renh@geo.vu.nl (H. Renssen).

0277-3791/03/$ - see front matter
PII: S0277-3791(02)00190-7

phases: the Early Pleniglacial (74–59 kyr BP), the Hasselo Stadial (41.5–40 kyr BP), the LGM and the Younger Dryas (~12.7–11.5 kyr BP) (Vandenberghe and Pissart, 1993; Huijzer and Isarin, 1997; Isarin, 1997; Huijzer and Vandenberghe, 1998). Obviously, the existence of active permafrost is evidence for mean annual temperatures well below 0°C, the details of which are discussed below.

In earlier studies we reported on various experiments on the Lateglacial climate performed with the Hamburg atmospheric general circulation model (AGCM) (e.g., Renssen, 1997). We tested this model's sensitivity to various changes in boundary conditions, such as vegetation distribution (Renssen and Lautenschlager, 2000) and SSTs/sea-ice cover (Renssen et al., 1996; Renssen, 1997). Moreover, we compared the results of these simulations with climate reconstructions based on terrestrial proxies to evaluate the model performance and to improve our understanding of the simulated climates (Isarin et al., 1997; Renssen and Isarin, 1998, 2001a,b; Isarin and Renssen, 1999; Renssen et al., 2000). In this paper we reverse the latter procedure, by using the AGCM's output to show that terrestrial proxies (in this case 'periglacial' data) may be applied to constrain the surface conditions of the North Atlantic (i.e. an AGCM boundary condition). To investigate the relation between permafrost conditions in NW Europe and sea-ice cover, we compare results of four experiments with different sea-ice extents.

2. Methods

2.1. Climate model and experimental design

2.1.1. The model

Our climate simulations were carried out with the ECHAM (European Centre/HAMburg) AGCM. This three-dimensional spectral model with 19 vertical layers is designed to simulate the atmospheric circulation at a subcontinental-to-global scale. We applied the so-called T42 version with a spatial resolution of $\sim 2.8^\circ \times 2.8^\circ$ latitude-longitude (DKRZ, 1994). Most results presented in this paper are from four experiments performed with the older ECHAM3 version, which produces a realistic modern climate (see Roeckner et al., 1992). In addition, we also present results of one experiment performed with the newer, up-dated version of the model, i.e. ECHAM4 (Roeckner et al., 1996). Considering the land-surface climate, the main improvement of ECHAM4 compared to ECHAM3 is a more appropriate representation of surface radiation fluxes, causing smaller errors in estimating temperature and precipitation (Roeckner et al., 1996). It should be noted that the representation of sea ice is relatively simple in the ECHAM model. When SSTs of less than −1.9°C are prescribed, the model assumes in the Northern Hemisphere a continuous sea ice cover with a thickness of 2 m. Using this thickness, the model calculates the heat flux between the ocean and atmosphere, on which the air temperature over the sea ice strongly depends. A sea-ice thickness of 2 m is a reasonable estimate for the Arctic Ocean, but is an overestimation near the sea-ice boundaries. Moreover, near the sea-ice margins it is likely that the cover is not continuous, as leads are normally present here, especially when strong surface winds are present. Probably, these two effects cause the model to overestimate the insulating effect of sea ice in a zone of a few 100 km (i.e. 1–2 grid cells, see e.g., Gloersen et al., 1992) near the sea-ice boundaries, resulting in too low surface air temperatures (i.e. a few °C difference, e.g., LeDrew and Barber, 1992; Parkinson et al., 2001).

2.1.2. Experimental design

The four palaeoclimate experiments presented in this study differ from a control simulation (CTRL) of the present-day climate by the definition of boundary conditions. These four palaeoclimate simulations may be characterised as follows (see also Table 1).

Table 1
Experimental design with the most important boundary conditions mentioned

Boundary conditions	Experiments				
	CTRL Modern	CATL Cold North Atlantic	YD1 'Younger Dryas'	YD2 'Younger Dryas cold'	LP 'Late Pleniglacial'
SSTs and sea ice	0 k	YD (N Atlantic)	YD (N Atlantic)	Summer: Atlantic as YD1 Winter: conveyor off −2°C in North Pacific	CLIMAP
Winter sea-ice limit Atl.	75°N	65°N	65°N	55–62°N	42–48°N
Ice sheets	0 k	0 k	12 k	12 k	15 k
Insolation	0 k	0 k	12 k	12 k	15 k
CO_2 (ppmv)	345	345	230	230	220

CTRL, CATL, YD1 and YD2 are performed with ECHAM3-T42, whereas LP is carried out with ECHAM4-T42. Here 'k' denotes cal kyr BP.

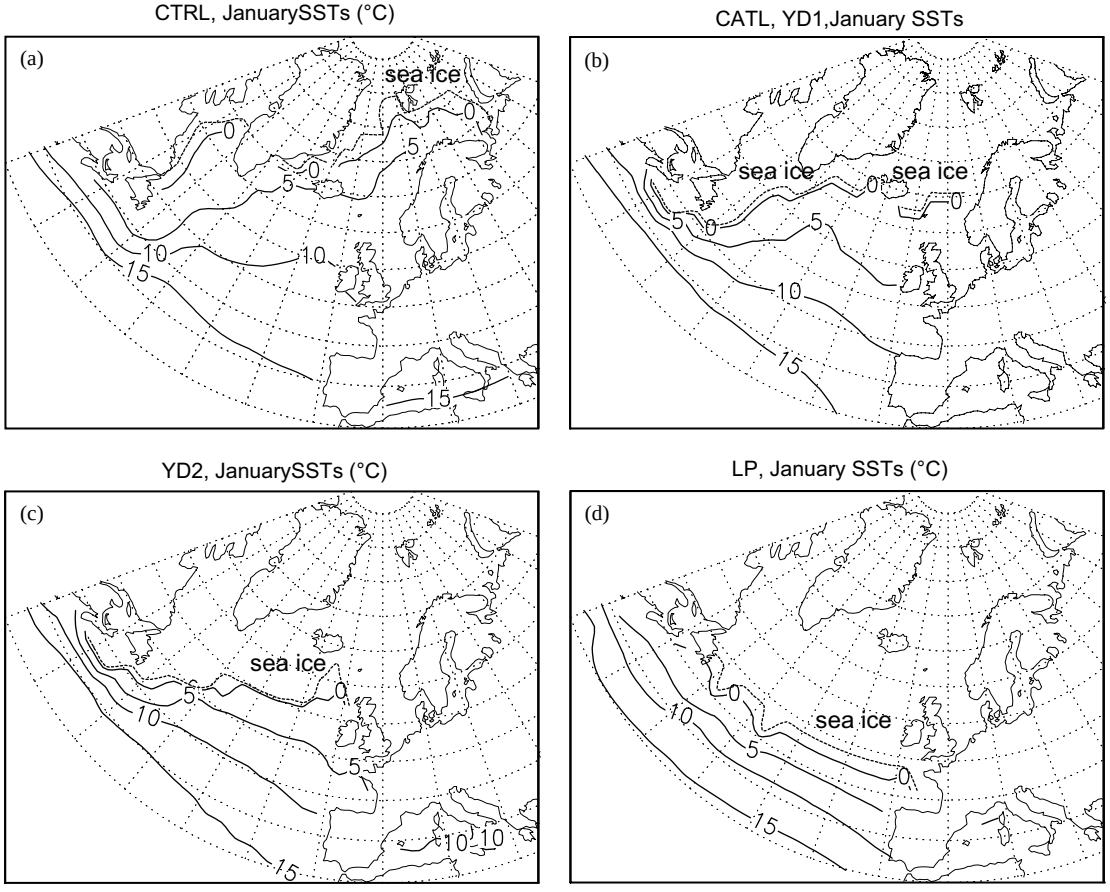

Fig. 1. Prescribed January ocean-surface conditions in the North Atlantic region. SSTs are plotted for 0°C, 5°C, 10°C and 15°C (solid lines). The broken line denotes the sea-ice margin (SST < -1.9°C). (a) CTRL (modern), (b) CATL and YD1 (based on Koç et al., 1993; Sarnthein et al., 1995), (c) YD2 (based on Schiller et al., 1997), (d) LP (based on CLIMAP, 1981).

(1) CATL: modern boundary conditions, but with a cold North Atlantic,
(2) YD1: Younger Dryas boundary conditions with a cold North Atlantic as in CATL,
(3) YD2: as YD1, but with additional ocean cooling in North Atlantic (winter only), inferred from comparing proxy data and model results (discussed in detail in Renssen, 1997), and
(4) LP: Late Pleniglacial boundary conditions.

The most important boundary conditions are ocean-surface conditions (SSTs and sea ice), extent and elevation of ice sheets, insolation and atmospheric concentration of CO_2 (Table 1). As our aim is to investigate the relation between European permafrost distribution and North Atlantic sea-ice cover, we present results of three experiments with different extents of sea-ice cover, viz. YD1, YD2 and LP. In these three experiments other boundary conditions (i.e., ice sheets, insolation and CO_2 concentration) are also changed relative to CTRL. In addition, we present results of a fourth experiment (CATL) with modern boundary conditions as in CTRL, except for the North Atlantic that is cooled as in YD1, enabling us to distinguish the effect of ocean-surface conditions from the other boundary conditions by comparing the results of CATL and YD1. Experiment LP was performed with ECHAM4. The sets of boundary conditions are detailed elsewhere (Renssen, 1997; Renssen and Isarin, 2001a) and summarised below.

2.1.3. Ocean-surface conditions

In the palaeoclimate experiments different magnitudes of ocean cooling are prescribed. Most importantly, the winter sea-ice margin shifts from 75°N in CTRL, to 65°N in CATL and YD1, 55–62°N in YD2 and 46–48°N in LP (Figs. 1a–d). The sea-ice cover in CATL and YD1 is based on palaeoceanographic reconstructions of Sarnthein et al. (1995) and Koç et al. (1993). A detailed model-data comparison suggested that Atlantic winter sea-ice cover was more extensive during the YD (see detailed discussion in Renssen et al., 1995; Renssen, 1997). Therefore, a second YD simulation (YD2) was performed with an additional Atlantic cooling (Fig. 1c) based on a conveyor belt shutdown in a

Table 2
Relation between various types of periglacial evidence and temperatures (simplified after Huijzer and Isarin, 1997)

Periglacial phenomena	Mean annual air temperature	Mean air temperature coldest month
Thermal contraction cracks		
Ice-wedge cast, relic sand wedge, composite-wedge cast	$\leqslant -4^{\circ}C$[a]	$\leqslant -20^{\circ}C$
	$\leqslant -8^{\circ}C$[b]	$\leqslant -20^{\circ}C$
Seasonal frost crack	$\leqslant -1^{\circ}C$ to $0^{\circ}C$	$\leqslant -8^{\circ}C$
Periglacial involutions		
Large-scale (amplitude $\geqslant 0.6$ m)	$\leqslant -4^{\circ}C$[a]	$\leqslant -20^{\circ}C$
	$\leqslant -8^{\circ}C$[b]	
Small-scale (amplitude < 0.6 m)	$\leqslant -1^{\circ}C$	
Perennial frost mounds		
Open-system pingo	$\leqslant -3^{\circ}C$ to $\leqslant -1^{\circ}C$	
Closed-system pingo	$\leqslant -6^{\circ}C$ to $\leqslant -4^{\circ}C$	
Organic palsa	$\leqslant -1^{\circ}C$	
Mineral palsa	$\leqslant -6^{\circ}C$ to $\leqslant -4^{\circ}C$	

[a] Some inferences are only valid for phenomena in fine-grained substrate (see Huijzer and Isarin, 1997) for all references.
[b] Some inferences are only valid for phenomena in coarse-grained substrate (see Huijzer and Isarin, 1997) for all references.

coupled atmosphere–ocean model experiment (Schiller et al., 1997). As suggested by Renssen and Isarin (1998), the prescribed sea-ice cover in YD2 may still underestimate the oceanic cooling that occurred during the YD. In the Late Pleniglacial experiment (LP) the global SST reconstructions of CLIMAP (1981) were prescribed, including an extensive North Atlantic cooling (Fig. 1d, Renssen and Isarin, 2001a, b).

2.1.4. Other boundary conditions: ice sheets, insolation and atmospheric CO_2

In YD1, YD2 and LP we altered the topography and surface albedo to account for the presence of the Scandinavian, British and Laurentide ice sheets (Renssen and Isarin, 2001a). Ice-sheet extents and elevations are based on reconstructions of Peltier (1994). A surface albedo of 0.8 was prescribed for these ice sheets, whereas the value ranges from 0.6 to 0.8 for the ice sheets in Antarctica and Greenland. Moreover, we changed the land–sea distribution by converting sea cells to land cells in the North Sea region to include the effect of a lower sea level (e.g., Fairbanks, 1989). Insolation was changed in YD1, YD2 and LP according to Berger (1978), leading in the northern hemisphere mid-latitudes to more incoming solar radiation during summer and less during winter. The atmospheric CO_2 concentration was lowered from 345 ppmv in CTRL to 230 ppmv (YD1 and YD2) and 220 ppmv (LP), based on analyses in Antarctic ice cores (e.g., Barnola et al., 1987). In addition, in LP we also lowered the concentrations of CH_4 and N_2O (Raynaud et al., 1993), a change not possible in the experiments (YD1 and YD2) carried out with the older model version (ECHAM3). Furthermore, the LP experiment also took into account the effect of different vegetation by changing the values of surface background albedo, leaf area index, vegetation cover, forest cover and roughness length (Claussen et al., 1994). The values of these parameters were altered according to the glacial vegetation reconstruction of Adams and Faure (1997), following the procedure detailed in Renssen and Lautenschlager (2000).

2.2. General principles of climate reconstruction in permafrost regions

Permafrost occurs when the subsoil that has been frozen in winter does not thaw completely in summer during at least two successive years. A distinction may be made between regions with continuous and discontinuous permafrost. The permafrost is called continuous when it occurs at all places. From studies in present-day periglacial environments it appears that the boundary between discontinuous and continuous permafrost depends on special temperature requirements, and on the lithology of the subsoil (Romanovskij, 1976) and the thickness of the snow cover. A mean annual air temperature (MAAT) below $-8^{\circ}C$ is required for regions with a sandy or gravely subsoil, while in regions with a fine-grained subsoil (e.g., loess) this temperature must be lower than $-4^{\circ}C$ (Vandenberghe and Pissart, 1993). It means that mean annual air temperatures between $-4^{\circ}C$ and $-8^{\circ}C$ produce continuous permafrost in loess regions, no permafrost in sandy-gravely regions, and discontinuous permafrost in regions with both fine and coarse-grained soils.

Various types of sedimentary deformation and landforms are characteristic of continuous or discontinuous permafrost (Table 2). Many of these phenomena have left distinct features in the geological archive and may

thus be used as evidence for the former existence of permafrost and the related temperature conditions. As shown in Table 2, three relevant types of periglacial features can be identified: (1) thermal contraction cracks, (2) periglacial involutions and (3) perennial frost mounds. Thermal contraction of the frozen ground due to lowering of the temperature often leads to the formation of so-called *thermal contraction cracks* (French, 1996). Due to repeated cracking, they may develop into wedges filled by ice or sand. They form only in continuous permafrost. Another type of crack is narrow and shallow and develops already in the seasonally frozen layer. It does not require the existence of permafrost. Degradation of ice-rich permafrost my lead to soil deformation (*periglacial* '*involutions*' or 'cryoturbations', Vandenberghe and Van de Broek, 1982; Murton et al., 1995). A distinction must be made between large-scale structures that require permafrost for their development, and smaller-scale cryoturbations that may form under seasonal frost (Vandenberghe, 1988). In permafrost environments *perennial frost mounds* may develop as an effect of the local freezing of soil water. Various types (i.e. pingos and palsas) are identified on the basis of the mechanism of formation and on the structure and properties of the ice inside the mounds (Mackay, 1978, 1988; French, 1996; Pissart et al., 1998).

3. Model results

3.1. Introduction

In Section 2.2 it was discussed that the southern limit of continuous permafrost represents a maximum mean annual air temperature of −8°C and a mean winter temperature lower than −20°C. Moreover, discontinuous permafrost only develops when mean annual temperatures are −4°C or below. In this section we focus on the relation between the same temperatures in the simulation results and the various prescribed ocean-surface conditions. But before we can establish this relation, we need to identify the effect of these ocean-surface conditions compared to that of other changed boundary conditions.

3.2. Impact of ocean-surface conditions vs. other boundary conditions

The effect of SSTs and sea ice compared to the composite effect of ice sheets, insolation and greenhouse gases is investigated by analysing the difference between CATL and YD1 (Table 1). As expected, compared to CTRL (Fig. 2a and b) the changes in boundary conditions caused a considerable change in air temperatures in CATL and YD1 (Figs. 3a and b and 4a and b). Moreover, a comparison of Figs. 3a and b and 4a and b reveals that mean January and annual isotherms are very similar in CATL and YD1. Consequently, it appears that ocean-surface conditions control the surface air temperature distribution in Europe. What is the effect of ice sheets, insolation and greenhouse gases on the temperature? In an earlier study we showed that the main impact of the Scandinavian ice sheet in YD1 was a cooling over its surface during summer (Renssen, 1997). This effect is visible in the mean annual temperature plot for YD1, as cooler conditions are simulated over Scandinavia compared to CATL (compare Fig. 4b with Fig. 3b). Moreover, in Renssen (1997) it was also shown that insolation caused summer warming of 1–2°C over continental Europe in YD1 compared to CATL. The impacts of lowered CO_2 concentration and insolation in winter were negligible in Europe (Renssen, 1997). In summary, we conclude that in YD1, YD2 and LP, the combined effect of ice sheets, insolation and greenhouse gases on the temperature distribution in Europe is minor compared to the dominating impact of ocean-surface conditions.

3.3. Relation between air temperatures and ocean-surface conditions

In the palaeoclimate simulations, the prescribed winter sea-ice margin is at the same latitude as the thermal limits associated with the southern margin of permafrost in NW Europe. The computed January air temperatures (Figs. 2a, 3a, 4a, 5a and 6a) over the prescribed Atlantic sea-ice cover (Figs. 1a–d) are below −15°C to −20°C. As expected, over the coastal region of NW Europe the latitude of the −15°C and −20°C isotherms is equivalent to the latitude of the prescribed southern sea-ice margin. Compared to CTRL, the winter isotherms in our palaeoclimate experiments are more zonally orientated due to the colder Atlantic Ocean. Moreover, near the European Atlantic coast the zone with simulated *annual* air temperatures between −4 and −8°C (i.e. discontinuous permafrost conditions) coincides within 5° of latitude with the computed −15°C and −20°C January isotherms (compare Figs. 3b, 4b, 5b and 6b with Figs. 3a, 4a, 5a and 6a). Consequently, in the model the *occurrence of permafrost conditions in NW Europe is controlled by the winter sea-ice limit in the North Atlantic Ocean*. As discussed, the representation of sea ice in the ECHAM model is relatively simplified, which could potentially lead to an overestimation of surface cooling over sea ice of a few degrees centigrade. Nevertheless, if we assume that the observed sea ice-permafrost relation is real, the procedure may be reversed by using reconstructions of permafrost distribution in NW Europe to constrain the sea-ice extent in the North Atlantic.

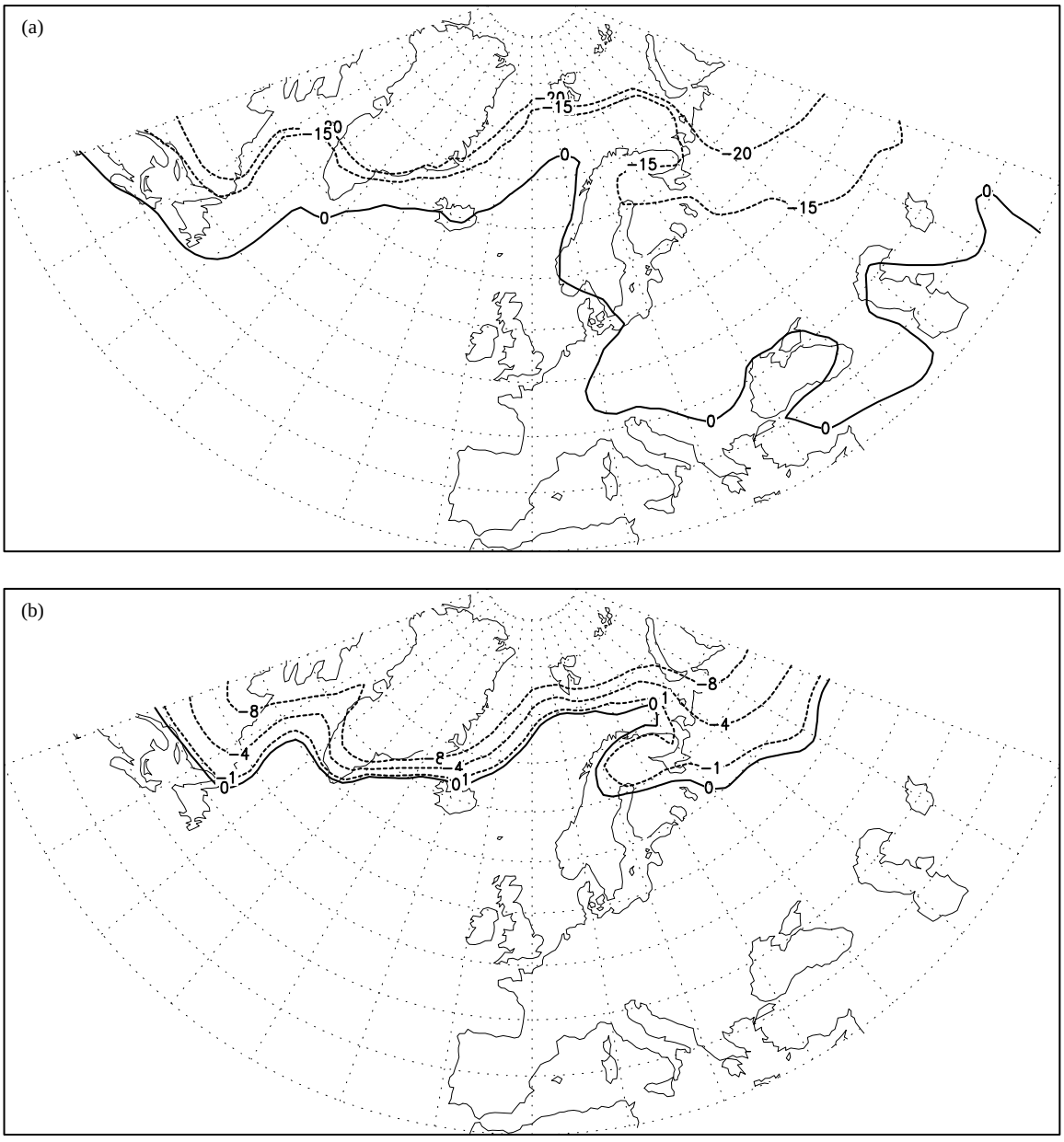

Fig. 2. Simulated maximum surface (2 m) air temperatures in °C for CTRL: (a) January, (b) annual. Shown are the isotherms that are associated with permafrost conditions. For the southern limits of continuous and discontinuous permafrost, the maximum annual air temperatures are −8°C and −4°C, respectively.

4. Permafrost distribution in Northwest and Central Europe

The permafrost distribution in northwest and central Europe is well known for the Last Glacial. Permafrost occurred during the Early Pleniglacial, Hasselo Stadial, LGM and YD. Between these periods, permafrost disappeared largely from the study region. Table 3 gives an overview of permafrost limits in NW Europe during these cold phases. Maps of permafrost distributions for various phases have been presented by Huijzer and Isarin (1997), Isarin (1997) and Huijzer and Vandenberghe (1998). Here we show the permafrost limits for the LGM and YD (Figs. 7a and 7b), as these two phases are discussed in detail.

4.1. Permafrost reconstructions for the LGM in NW and Central Europe

After the relatively warm MIS 3, permafrost re-established during the LGM after 28 kyr BP (Fig. 7a). Huijzer and Vandenberghe (1998) made an extensive inventory of all described permafrost relics from that period in northwest and central Europe. From

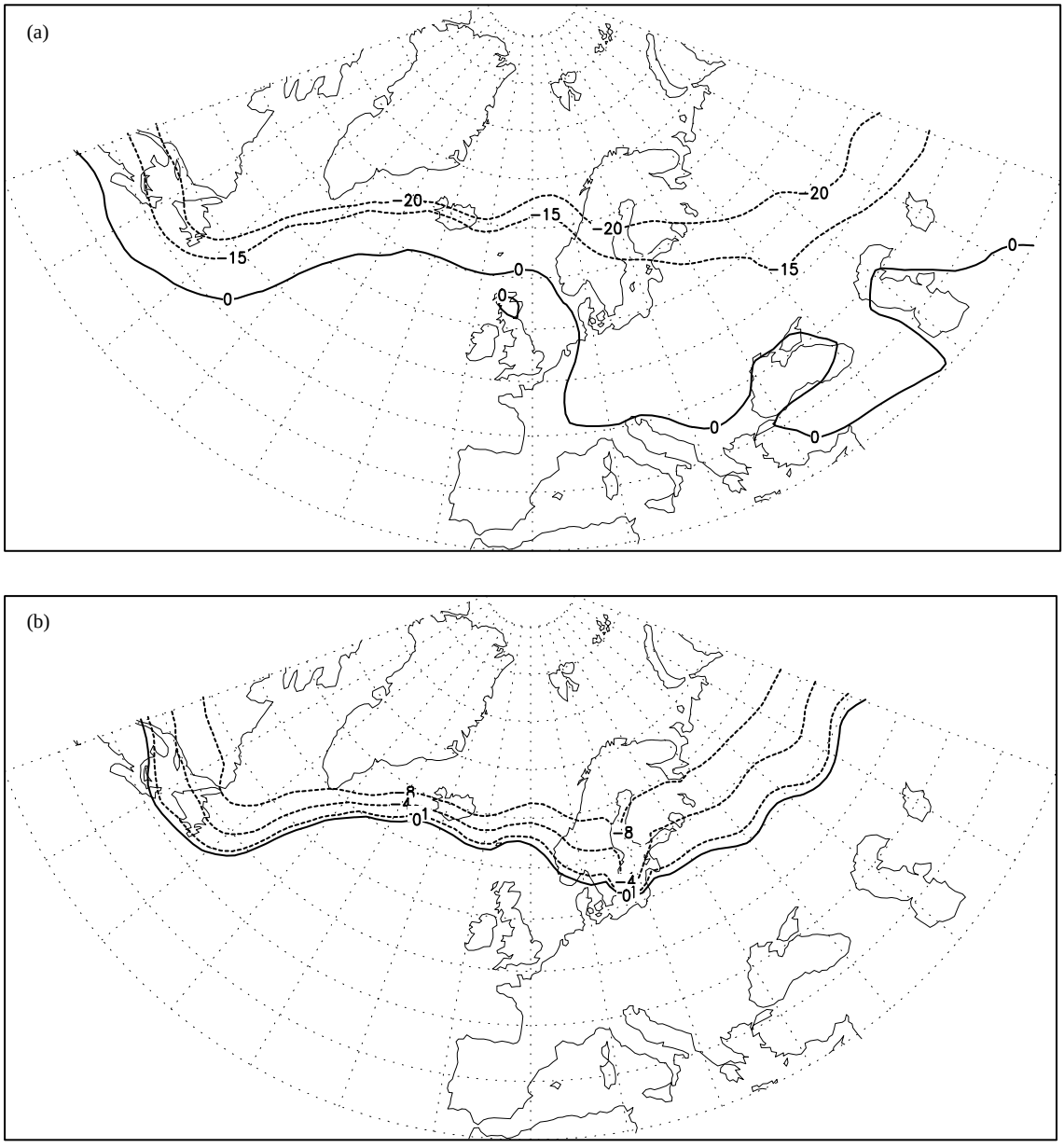

Fig. 3. Simulated maximum surface air temperatures in °C for CATL: (a) January, (b) annual. Shown are the isotherms that are associated with permafrost conditions. For the southern limits of continuous and discontinuous permafrost, the maximum annual air temperatures are −8°C and −4°C, respectively.

their map it is clear that continuous permafrost extended throughout the UK, northern Belgium, The Netherlands and northern Germany and Poland. The latter authors put the boundary with the discontinuous permafrost zone around the Belgian–French border. This is in contrast with the map of Van Vliet-Lanoë (1996), showing continuous permafrost also over northern, central and eastern France. The very cold conditions in central and eastern France as reconstructed by Van Vliet-Lanoë (1996) may be due to their higher altitude, and it should be noted that the permafrost reconstructions by Huijzer and Vandenberghe (1998) represent the situation reduced to sea level. Furthermore, the north–south boundary between continuous and discontinuous permafrost by Van Vliet-Lanoë (1996) over central France is not compatible with the clear and strong dominance of N–S gradients in all the coldest periods of the Last Glacial (Coope et al., 1998; Huijzer and Vandenberghe, 1998; Isarin et al., 1998). Invoking a strong influence by a 'warmer' Atlantic Ocean to explain the supposed W–E gradient does not conform with the evidence.

For the present study it should be emphasised that the reconstructions of the palaeoclimatic conditions in western France are similar in both approaches. Notwithstanding the differences in central and eastern

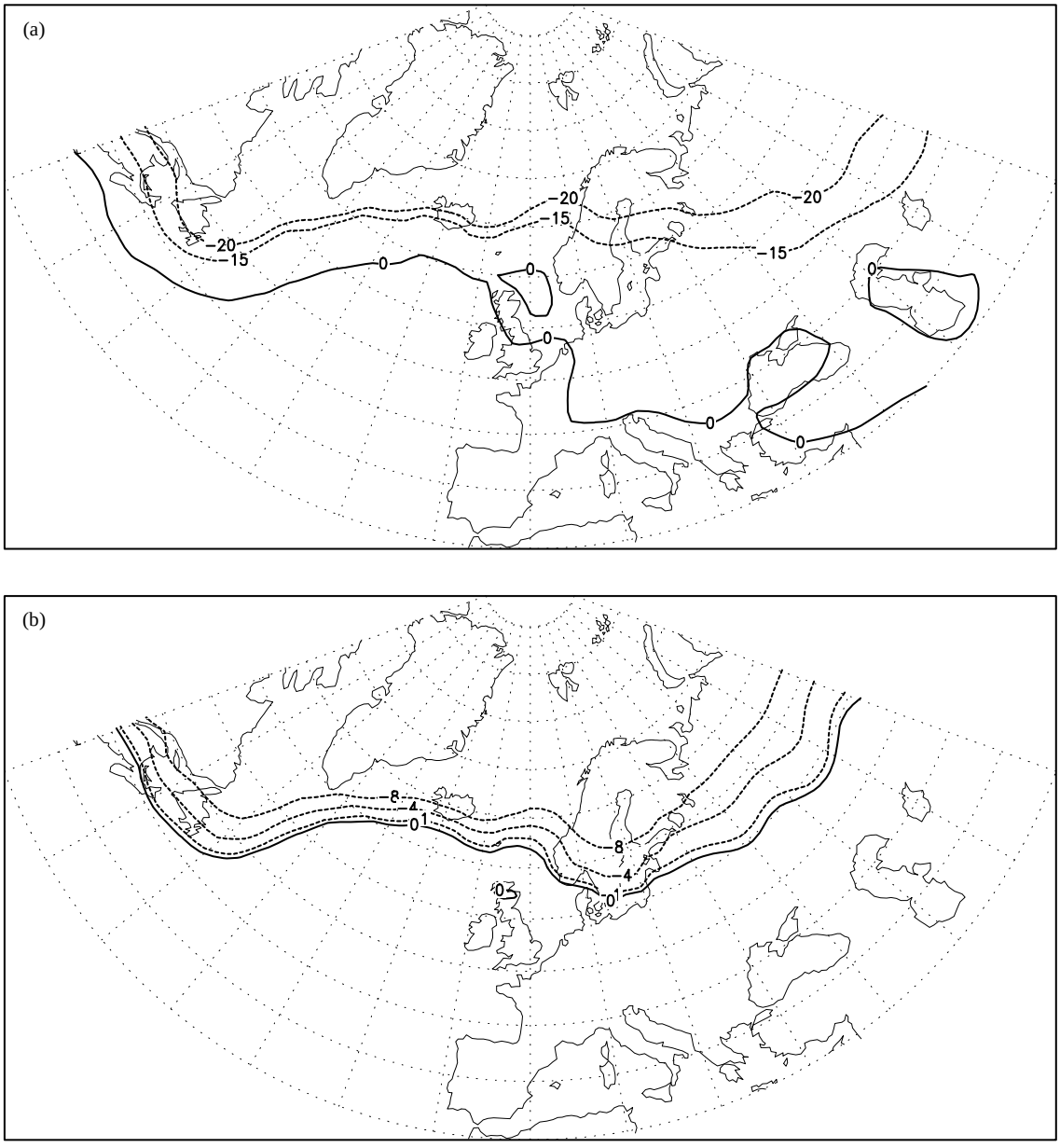

Fig. 4. Simulated maximum surface air temperatures in °C for YD1: (a) January, (b) annual. Shown are the isotherms that are associated with permafrost conditions. For the southern limits of continuous and discontinuous permafrost, the maximum annual air temperatures are −8°C and −4°C, respectively.

France described above, both reconstructions put the continuous–discontinuous permafrost boundary (equivalent with a mean annual air temperature of −8°C) on the continental shelf at 50°N (Fig. 7a). Corresponding temperatures of the coldest month should have been around −25°C (Huijzer and Vandenberghe, 1998). These winter temperatures agree with data based on beetle occurrences. Assuming a (nearly) symmetrical annual temperature cycle, with a mean annual temperature of −8°C and a summer temperature of +8°C (Vandenberghe, 1985a), also gives winter temperatures around or less than −25°C, which is in agreement with data based on beetle occurrences (Huijzer and Vandenberghe, 1998). To conclude, in the present study we combine the permafrost reconstructions of Van Vliet-Lanoë (1996) and Huijzer and Vandenberghe (1998), resulting in the map presented in Fig. 7a.

The described temperature conditions characterise the coldest episodes of the LGM. In Belgium and The Netherlands (Fig. 8) there are a few indications that the ice wedges in sandy subsoils degraded temporarily around 22–21 kyr BP, but resumed their development afterwards (e.g., Vandenberghe, 1977; Van Huissteden et al., 2000). It has not been proven that this permafrost degradation had a climatic origin, but it is also not

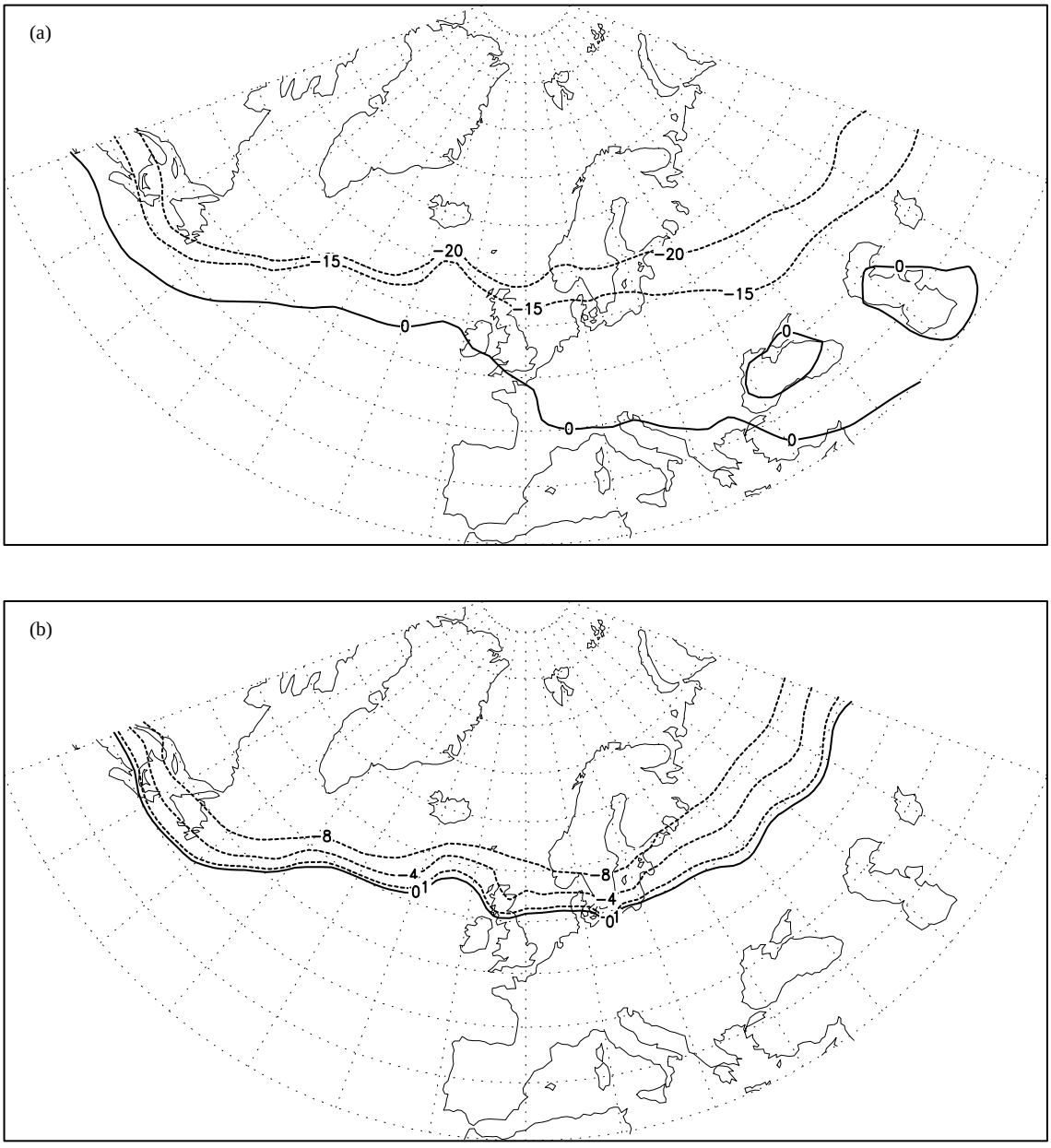

Fig. 5. Simulated maximum surface air temperatures in °C for YD2: (a) January, (b) annual. Shown are the isotherms that are associated with permafrost conditions. For the southern limits of continuous and discontinuous permafrost, the maximum annual air temperatures are −8°C and −4°C, respectively.

excluded that this phase corresponded with a warmer oscillation in the Greenland ice-core records. Finally, continuous permafrost disappeared after 20 kyr BP in the coversand region of The Netherlands (Bateman and van Huissteden, 1999). Within the loess substratum in Belgium ice wedges persisted for some longer time since the degradation of the youngest ice wedges took place just before 17 kyr BP (based on luminescence and radiocarbon dates: Vandenberghe, 1985b; Vandenberghe et al., 1998; Van den Haute et al., 1998). It means that the permafrost zone shifted rapidly northwards after 20 kyr BP. Between 15 and 17 kyr BP, a narrow zone with continuous permafrost (evidenced by the occurrence of ice-wedge casts) persisted only near to the retreating ice sheets (e.g., in Poland and northernmost Germany: Kozarski, 1993; Helbig, 1999). In The Netherlands and Belgium deep frost cracks developed in that period pointing to mean annual air temperatures below −1°C (Fig. 8).

4.2. Permafrost reconstruction for the Weichselian Lateglacial in NW and Central Europe

In the relatively warm period preceding the Younger Dryas (i.e. Bølling-Allerød Interstadial or Greenland Interstadial 1), there were no indications at all for

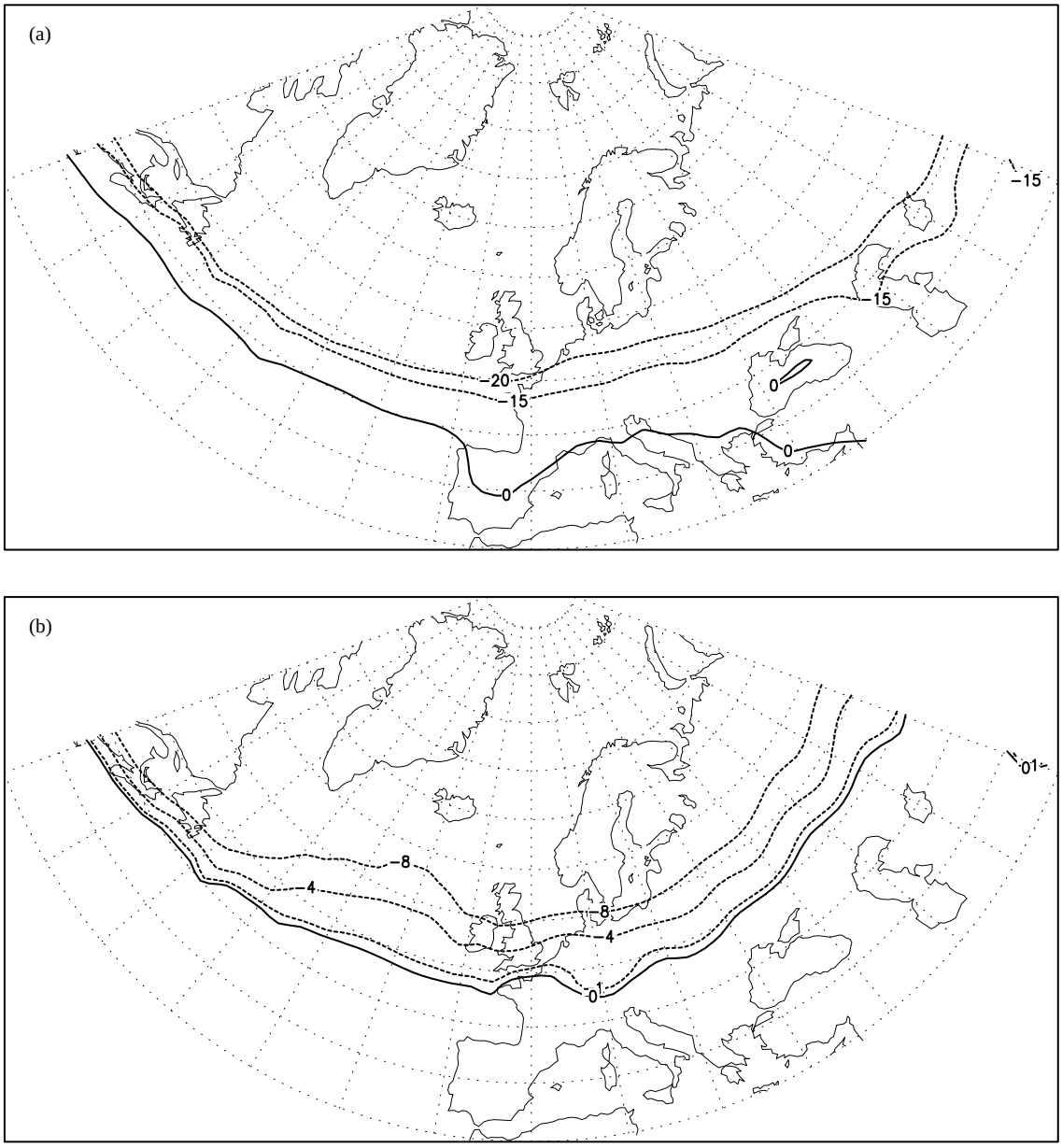

Fig. 6. Simulated maximum surface air temperatures in °C for LP: (a) January, (b) annual. Shown are the isotherms that are associated with permafrost conditions. For the southern limits of continuous and discontinuous permafrost, the maximum annual air temperatures are −8°C and −4°C, respectively.

permafrost conditions in The Netherlands and Belgium (Vandenberghe and Pissart, 1993). Mean annual air temperatures rose even considerably above 0°C at the beginning of this period (Renssen and Isarin, 2001a).

For the Younger Dryas, Isarin (1997) and Isarin et al. (1998) defined the southern boundaries of the continuous and the discontinuous permafrost, corresponding, respectively, with the −8° and −4°C isotherms of mean annual air temperature (Fig. 7b). The results show a northward shift of about 5° for the E–W trending −8°C isotherm, going through central Ireland (ca 55°N), in comparison with the same isotherm during the coldest part of the LGM (Fig. 7a). A similar northward shift of the −4°C isotherm is derived, going through the southernmost part of England (ca 50°N). The latter line should correspond approximately with the −20°C isotherm of the coldest winter month.

4.3. Summary

Extensive periglacial evidence shows that during the 4 cold phases in the Last Glacial permafrost was present in NW Europe as far south as 50°N. Following the observation that the latitude of permafrost extension in NW Europe is controlled by the winter sea-ice cover (Section 3), this suggests that the Atlantic Ocean was

Table 3
Latitudes of southern margins of discontinuous and continuous permafrost in NW Europe for several cold glacial phases

Cold phase	Latitude discontinuous permafrost	Latitude continuous permafrost
Younger Dryas (12.9–11.5 k)	50°N	55°N
LGM (23–19 k)	45°N?	50°N
Hasselo stadial (41.5–40 k)	50°N	55°N
Early Pleniglacial (phases within 74–59 k)	45°N?	50°N

Margins are taken from Huijzer and Isarin (1997), Isarin (1997) and Huijzer and Vandenberghe (1998), and are based on numerous sites with periglacial features ('k' denotes cal kyr BP).

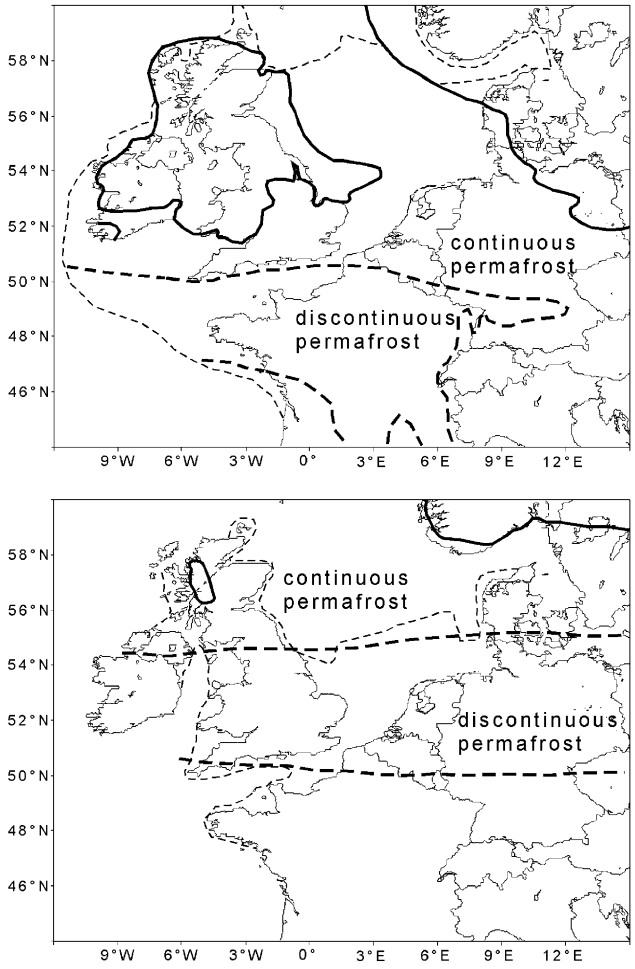

Fig. 7. Map of permafrost limits in NW Europe for: (a) the phase of maximum cold (24–21 kyr BP, based on Huijzer and Isarin, 1997; Huijzer and Vandenberghe, 1998; Van Vliet-Lanoë, 1996), (b) the Younger Dryas (based on Isarin, 1997). Thick continuous line = limits of ice sheets, thick dashed line = permafrost limits, thin dashed line = shore limits. In Fig. 7a, permafrost in Italy is not considered due to a lack of data, whereas in Fig. 7b, the upland permafrost south of 50°N is not taken into account. The southern margins of continuous and discontinuous permafrost correspond to maximum annual air temperatures of −8°C and −4°C, respectively.

covered by sea ice southwards to 50°N during at least the 4 cold glacial phases in Table 3. As permafrost evolves as a reaction to mean climate conditions, this inferred sea-ice cover must be considered as representing the mean winter state in the North Atlantic during these cold periods. How do these inferred sea-ice conditions compare with North Atlantic evidence from palaeoceanographic proxies?

5. Comparison palaeoceanographic evidence and European permafrost conditions

The period with maximum cold on the West European continent (23–19 kyr BP) is quite similar in timing to the LGM recognised in North Atlantic Ocean sediments as a $\delta^{18}O$ minimum around ~21 cal kyr BP (i.e. maximum in global ice volume, Mix et al., 2001; Clark and Mix, 2002; Waelbroeck et al., 2002). In palaeoceanographical literature, the LGM is considered to fall between Heinrich (H) events 1 and 2 (Bard et al., 2000; de Vernal et al., 2000; Sarnthein et al., 2000). The H events themselves are oceanic events, i.e. periods with enhanced ice-rafted transport of detrital carbonate to the North Atlantic (Bond et al., 1997, 1999). According to Sarnthein et al. (2000), the H2 and H1 events have chronological limits of 23.4–24.2 and 18.1–14.7 kyr BP, respectively.

In recent literature, three basic modes of Atlantic Ocean circulation are recognised (e.g., Alley et al., 1999; Sarnthein et al., 2000): (1) interglacial mode, with a strength of thermohaline circulation comparable to today, (2) glacial mode, with reduced deep-water formation (by 30–50%), and (3) a Heinrich meltwater mode with a switched-off thermohaline circulation. These three modes have characteristic patterns of ocean-surface cooling and sea-ice cover that have been reconstructed using palaeoceanographic proxies. It should be stressed that we focus here on the *mean* oceanic conditions that can be considered to represent equivalent time scales as the reconstructed permafrost distributions.

The glacial mode prevailed during the LGM and is characterised by a considerable difference between summer and winter conditions, especially in the Nordic Seas. Here, an extensive sea-ice cover was only formed in winter, as the inflow of relatively warm water along the Norwegian coast produced summer SSTs of 4°C. Different views exist on the actual extent of the winter

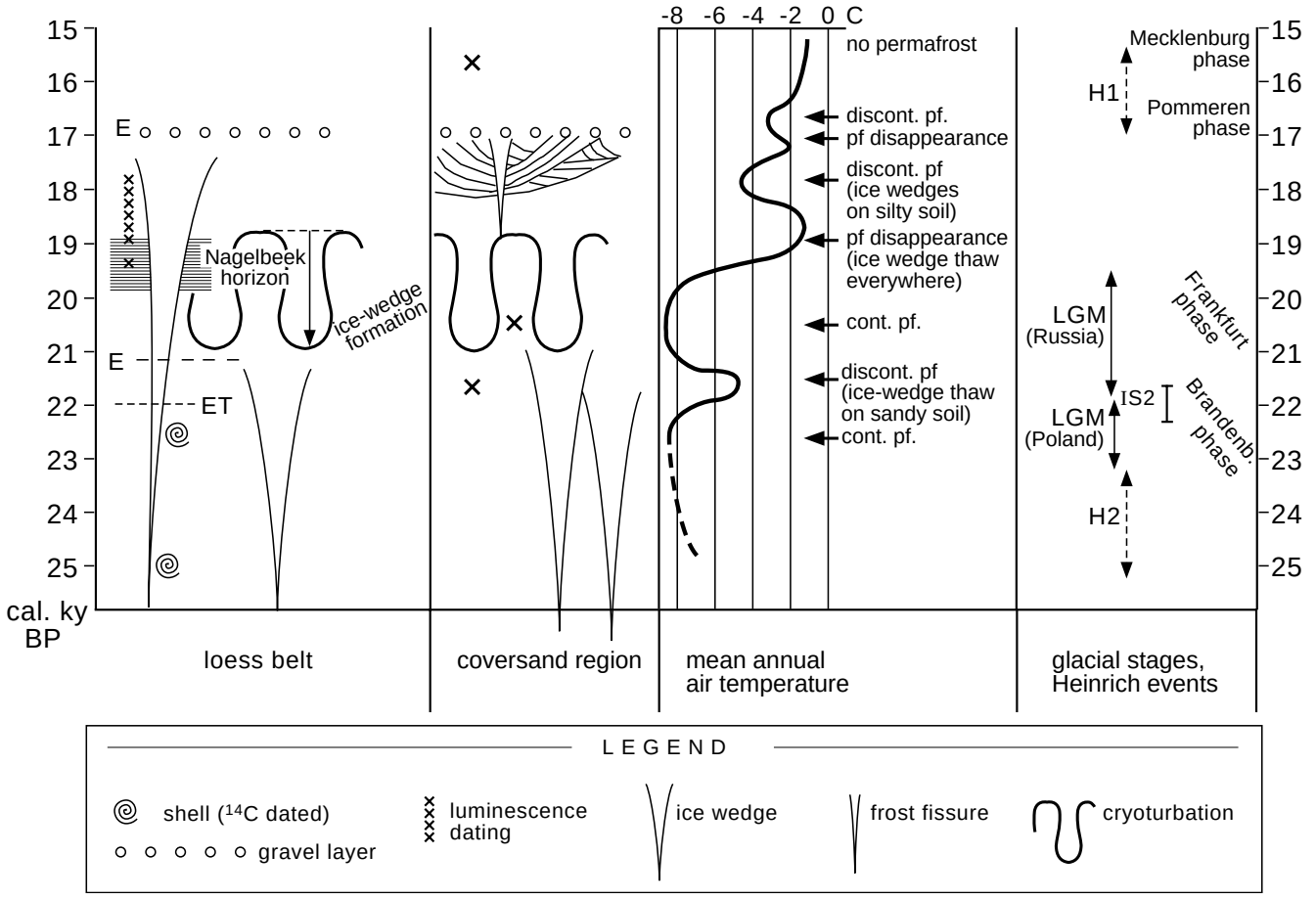

Fig. 8. The period after the LGM in the Dutch–Belgian region (50–53°N): permafrost occurrence, mean annual temperature (in °C) and periglacial phenomena, with representation of main glacial advances and Heinrich events; plotted against time in cal kyr BP. Also Van Vliet-Lanoë (1992) recognised a general warming after the formation of the Nagelbeek horizon, although her chronology is somewhat different. ET signifies Eltville Tuff (volcanic ash layer), erosion levels are given by E, and IS is interstadial.

sea-ice cover in the central North Atlantic Ocean. The original reconstruction of CLIMAP (1981), based on foraminifera, included an ice-covered Atlantic ocean southwards to 45°N. Sarnthein et al. (2000) seem to agree with these winter conditions as they state: "we conclude that a continuous CLIMAP (1981)-style sea-ice cover occurred during glacial winter only". In contrast, in an overview study based on dinoflagellates, deVernal et al. (2000) conclude that the central North Atlantic must have been perennially ice-free during the LGM. Sarnthein et al. (2000) explain the strong contrast between summer and winter by the formation of deepwater during summer instead of winter as in the modern climate. Reconstructions of sea-surface salinities for the LGM suggest that the summer salinities may have had sufficiently high values in the central Atlantic to make deepwater formation possible. This concept would be consistent with our inferences of an extensive winter sea-ice cover in the North Atlantic Ocean. Moreover, it would agree with relatively high continental summer temperatures during the LGM (e.g., Kolstrup, 1980).

In the Heinrich meltwater mode a permanent sea-ice cover in the Nordic Seas is associated with the collapsed thermohaline circulation. To our knowledge, no specific reconstruction of North Atlantic surface conditions exists for the H2 and H4 events. For the H1 event, Sarnthein et al. (2000) placed the winter sea-ice limit between 55°N (close to Scotland) and 60°N (South of Iceland, i.e. with a SE–NW orientation), leaving the central North Atlantic ice-free. This may be a conservative estimate, as Sarnthein et al. (2000) note that the exact winter sea-ice limits are still uncertain. In any case, this winter sea-ice cover based on palaeoceanographical proxies is positioned much further to the North than our estimates for the LGM.

Compared to the H-events and the LGM, the position of the YD is somewhat special, as it occurred in the middle of the last deglaciation. According to Sarnthein et al. (2000), in the early part of the YD (i.e. 12.7–11.8 kyr BP) the North Atlantic Ocean circulation resembled the present state (modern mode 1), whereas during the later part a meltwater event caused a

switch to mode 3 (Heinrich mode) with a collapsed thermohaline circulation. The foraminifera-based reconstruction of Sarnthein et al. (2000) for the early YD suggests for winter a sea-ice limit at 65°N (i.e. ice-covered Nordic seas) and SSTs varying between 2 and 9°C at 55–60°N. Consequently, the latter YD reconstruction is similar to the one prescribed in experiment YD1 (Fig. 1b, after Sarnthein et al., 1995). However, this view of the surface conditions during the YD is obviously in conflict with our inferences based on periglacial data, as the winter sea-ice limits are 15 latitudinal degrees apart (i.e. 65°N vs. 50°N).

6. Implications of our results

Some reconstructions of ocean-surface conditions based on marine proxies are clearly inconsistent with our inferred extended sea-ice cover in the North Atlantic. This is especially clear for the YD, and to a lesser extent for full-glacial conditions. What is causing this clear inconsistency between periglacial data and marine proxies? One explanation could be that many Atlantic Ocean cores have insufficient temporal resolution to capture the coldest spike of cooling events, which may last only a few hundred years such as in the case of the YD. Another reason might be that the relation between particular oceanic proxies and ocean winter surface conditions is less straightforward than presumed (e.g., Mix et al., 2001). In particular, the relatively warm glacial Atlantic Ocean as reconstructed using dino-cysts (de Vernal et al., 2000) appears incompatible with our inferences. Alternatively, the inferred relation between Atlantic winter sea-ice cover and permafrost distribution in Western Europe is more complex than suggested here. The derivation of mean annual temperatures from periglacial proxies supposedly does not deviate by more than a few degrees centigrade because of the reliability of the modern analogue principle in this case (Romanovskij, 1976; Mackay, 1978, 1988; Pissart et al., 1998). Further research is clearly required to shed more light on this issue, especially on the apparent inconsistency between terrestrial and oceanic proxies during cold glacial phases.

7. Conclusions

1. An atmospheric general circulation model was used to perform several experiments in which different North Atlantic sea-ice extents were prescribed. The results of these simulations were compared with annual mean temperatures associated with southern limits of continuous permafrost (−8°C) and discontinuous permafrost (−4°C). This comparison suggests that the Late Quaternary distribution of permafrost in northwestern Europe was controlled by the position of the North Atlantic winter sea-ice margin. We propose that this relation may be applied to constrain the North Atlantic winter sea-ice extent during various cold glacial phases, using reconstructions of permafrost distribution. According to this approach, we find the following mean winter sea-ice margins in the North Atlantic Ocean:

- Early Pleniglacial: 50°N
- Hasselo Stadial: 50°N
- LGM: 45°N
- Younger Dryas: 50°N

2. For the Younger Dryas, our estimation of mean North Atlantic winter sea-ice conditions are in conflict with published estimates based on marine proxies (Sarnthein et al., 1995, 2000). In the latter reconstructions, an ice-free North Atlantic is proposed, which is incompatible with terrestrial evidence for permafrost conditions during the YD in Western Europe.

3. The proposed winter sea-ice margin for the LGM is similar to the original CLIMAP (1981) reconstruction. Thus, our inferences disagree with data from de Vernal et al. (2000) that suggest a perennially ice-free North Atlantic Ocean.

4. The reason for the discrepancy between periglacial data and marine proxy records is not clear yet. If our analysis is correct, this could suggest that the relation between particular oceanic proxies and winter ocean-surface conditions is less straightforward than presumed. In addition, in some cases, the temporal resolution of ocean cores could be insufficient to capture relatively short cold phases, such as the Younger Dryas.

5. Accepting our inferred extensive winter sea-ice extents supports the idea that the thermohaline circulation was significantly weakened or shutdown in winter during cold glacial phases. As suggested by Sarnthein et al. (2000), deepwater formation could have taken place during summer. This would be in agreement with certain proxies that indicate that the thermohaline circulation was active during the Younger Dryas and LGM.

Acknowledgements

The useful comments of J. Rose, T. Fichefet and two anonymous referees are gratefully acknowledged. The authors are indebted to L. Bengtsson (Max Planck Institute for Meteorology, Hamburg) and M. Lautenschlager (German Climate Computer Centre, Hamburg) for supporting the climate model experiments.

References

Adams, J.M., Faure, H., 1997. (Eds.), Review and Atlas of Palaeovegetation: Preliminary land Ecosystem Maps of the World since the Last Glacial Maximum. Oak Ridge National Laboratory, TN, USA. http://www.esd.ornl.gov/ern/qen/adams1.html.

Alley, R.B., Clark, P.U., Keigwin, L.D., Webb, R.S., 1999. Making sense of millennial-scale climate change. In: Clark, P.U., Webb, R.S., Keigwin, L.D. (Eds.), Mechanisms of Global Climate Change at Millennial Time Scales, Geophysical Monograph, Vol. 112, pp. 385–394. American Geophysical Union, Washington, D.C.

Bard, E., Rostek, F., Turon, J.-L., Gendreau, S., 2000. Hydrological impact of Heinrich events in the Subtropical Northeast Atlantic. Science 289, 1321–1324.

Barnola, J.M., Raynaud, D., Korotkevich, Y.S., Lorius, C., 1987. Vostok ice core provides 160,000-year record of atmospheric CO_2. Nature 329, 408–414.

Bateman, M.D., van Huissteden, J., 1999. The timing of last glacial periglacial and aeolian events, Twente, eastern Netherlands. Journal of Quaternary Science 14, 277–283.

Berger, A.L., 1978. Long-term variations of daily insolation and Quaternary climatic changes. Journal of the Atmospheric Sciences 35, 2363–2367.

Bond, G., Showers, W., Cheseby, M., Lotti, R., Almasi, P., deMenocal, P., Priore, P., Cullen, H., Hajdas, I., Bonani, G., 1997. A pervasive millennial-scale cycle in North Atlantic Holocene and Glacial climates. Science 278, 1257–1266.

Bond, G.C., Showers, W., Elliot, M., Evans, M., Lotti, R., Hajdas, I., Bonani, G., Johnsen, S., 1999. The North Atlantic's 1–2 kyr climate rhythm: relation to Heinrich events, Dansgaard/Oeschger cycles and the Little Ice Age. In: Clark, P.U., Webb, R.S., Keigwin, L.D. (Eds.), Mechanisms of Global Climate Change at Millennial Time Scales, Geophysical Monograph, Vol. 112, pp. 35–58. American Geophysical Union, Washington, D.C.

Broecker, W.S., 1998. Paleocean circulation during the last deglaciation: a bipolar seasaw? Paleoceanography 13, 119–121.

Clark, P.U., Mix, A.C., 2002. Ice sheets and sea level of the Last Glacial Maximum. Quaternary Science Reviews 21, 1–7.

Claussen, M., Lohmann, U., Roeckner, E., Schulzweida, U., 1994. A global data set of land-surface parameters. Report no. 135, Max-Planck-Institut für Meteorologie, Hamburg, 30pp.

CLIMAP project members, 1981. Seasonal reconstructions of the earth's surface at the Last Glacial Maximum. Geological Society of America Map and Chart Series MC-36.

Coope, G.R., Lemdahl, G., Lowe, J.J., Walkling, A., 1998. Temperature gradients in northern Europe during the last glacial-Holocene transition (14–9 ^{14}C kyr BP) interpreted from coleopteran assemblages. Journal of Quaternary Science 13, 419–433.

deVernal, A., Hillaire-Marcel, C., Turon, J.L., Matthiessen, J., 2000. Reconstruction of sea-surface temperature, salinity, and sea-ice cover in the northern North Atlantic during the Last Glacial Maximum based on dinocyst assemblages. Canadian Journal of Earth Sciences 37, 725–750.

DKRZ, 1994. The ECHAM 3 Atmospheric General Circulation Model. Technical Report no. 6, Deutsches Klimarechenzentrum Hamburg, 184pp.

Fairbanks, R.G., 1989. A 17,000-year glacio-eustatic sea level record: influence of glacial melting rates on the Younger Dryas event and deep-ocean circulation. Nature 342, 637–642.

French, H.M., 1996. The periglacial environment, 2nd Edition. Longman, Harlow, 341pp.

Gloersen, P., Campbell, W.J., Cavalieri, D.J., Comiso, C.L., Parkinson, C.L., Zwally, H.J., (1992). Arctic and Antarctic sea ice 1978–1987: satellite passive-microwave observations and analysis. National Aeronautics and Space Administration, 290pp.

Helbig, H., 1999. Die periglaziäre Überprägung der Grundmoränenplatten in Vorpommern. Petermanns Geographische Mitteilungen 143, 373–386.

Huijzer, A.S., Isarin, R.F.B., 1997. The reconstruction of past climates using multi-proxy evidence: an example of the Weichselian Pleniglacial in northwestern and central Europe. Quaternary Science Reviews 16, 513–533.

Huijzer, A.S., Vandenberghe, J., 1998. Climatic reconstruction of the Weichselian Pleniglacial in northwestern and central Europe. Journal of Quaternary Science 13, 391–417.

Isarin, R.F.B., 1997. Permafrost distribution and temperatures in Europe during the Younger Dryas. Permafrost and Periglacial Processes 8, 313–333.

Isarin, R.F.B., Renssen, H., 1999. Reconstructing and modelling Late Weichselian climates: the Younger Dryas in Europe as a case study. Earth-Science Reviews 48, 1–38.

Isarin, R.F.B., Renssen, H., Koster, E.A., 1997. Surface wind climate during the Younger Dryas in Europe as inferred from aeolian records and model simulations. Palaeogeography, Palaeoclimatology, Palaeoecology 134, 127–148.

Isarin, R.F.B., Renssen, H., Vandenberghe, J., 1998. The impact of the North Atlantic Ocean on the Younger Dryas climate in North-Western and Central Europe. Journal of Quaternary Science 13, 447–453.

Kitagawa, H., van der Plicht, J., 1998. Atmospheric radiocarbon calibration to 45,000 yr BP: Late Glacial fluctuations and cosmogenic isotope production. Science 279, 1187–1190.

Koç, N., Jansen, E., Haflidason, H., 1993. Paleoceanographic reconstructions of surface ocean conditions in the Greenland, Iceland and Norwegian Seas through the last 14 ka based on diatoms. Quaternary Science Reviews 12, 115–140.

Kolstrup, E., 1980. Climate and stratigraphy in northwestern Europe between 30.000 B.P. and 13.000 B.P., with special reference to the Netherlands. Mededelingen Rijks Geologische Dienst 32, 181–253.

Kozarski, S., 1993. Late Plenivistulian deglaciation and the expansion of the periglacial zone in NW Poland. Geologie en Mijnbouw 72, 143–157.

LeDrew, E.F., Barber, D.G., 1992. Snow, sea ice and climate: a study of scales. In: Woo, M.K., Gregor, D.J. (Eds.), Arctic Environment: Past, Present and Future. McMaster University, Hamilton, pp. 45–60.

Mackay, J.R., 1978. Contemporary pingos: a discussion. Biuletyn Peryglacjalny 27, 133–154.

Mackay, J.R., 1988. Pingo collapse and paleoclimate reconstruction. Canadian Journal of Earth Sciences 25, 495–511.

Manabe, S., Stouffer, R.J., 1997. Coupled ocean–atmosphere model response to freshwater input: comparison to Younger Dryas event. Paleoceanography 12, 321–336.

Martinson, D., Pisias, N.G., Hays, J.D., Imbrie, J., Moore, T.C., Shackleton, N.J., 1987. Age dating and the orbital theory of ice ages: development of a high-resolution 0 to 300,000-year chronostratigraphy. Quaternary Research 27, 1–30.

Mix, A.C., Bard, E., Schneider, R., 2001. Environmental processes of the ice age: land oceans, glaciers (EPILOG). Quaternary Science Reviews 20, 627–657.

Murton, J.B., Whiteman, C.A., Allen, P., 1995. Involutions in the Middle Pleistocene (Anglian) Barham soil, eastern England—a comparison with thermokarst involutions from Arctic Canada. Boreas 24, 269–280.

Parkinson, C.L., Rind, D., Healy, R.J., Martinson, D.G., 2001. The impact of sea ice concentration accuracies on climate model simulations with the GISS GCM. Journal of Climate 14, 2606–2623.

Peltier, W.R., 1994. Ice age paleotopography. Science 265, 195–201.

Pinot, S., Ramstein, G., Marsiat, I., de Vernal, A., Peyron, O., Duplessy, J.C., Weinelt, M., 1999. Sensitivity of the European

LGM climate to North Atlantic sea-surface temperature. Geophysical Research Letters 26, 1893–1896.

Pissart, A., Harris, S., Prick, A., Van Vliet-Lanoë, B., 1998. La signification paleoclimatique des lithalsas (palsas minérales). Biuletyn Peryglacjalny 37, 141–154.

Raynaud, D., Jouzel, J., Barnola, J.M., Chappellaz, J., Delmas, R.J., Lorius, C., 1993. The ice record of greenhouse gases. Science 259, 926–933.

Renssen, H., 1997. The global response to Younger Dryas boundary conditions in an AGCM simulation. Climate Dynamics 13, 587–599.

Renssen, H., Isarin, R.F.B., 1998. Surface temperature in NW Europe during the Younger Dryas: AGCM simulation compared with temperature reconstructions. Climate Dynamics 14, 33–44.

Renssen, H., Isarin, R.F.B., 2001a. The two major warming phases of the last deglaciation at ~14.7 and ~11.5 kyr cal BP in Europe: climate reconstructions and AGCM experiments. Global and Planetary Change 30, 117–153.

Renssen, H., Isarin, R.F.B., 2001b. Data-model comparison of the Younger Dryas event: discussion. Canadian Journal of Earth Sciences 38, 477–478.

Renssen, H., Lautenschlager, M., 2000. The effect of vegetation in a climate model simulation on the Younger Dryas. Global and Planetary Change 26, 423–443.

Renssen, H., Lautenschlager, M., Bengtsson, L., Schulzweida, U., 1995. AGCM experiments on the Younger Dryas climate. Report no. 173, Max-Planck-Institut für Meteorologie, Hamburg, 43pp.

Renssen, H., Lautenschlager, M., Schuurmans, C.J.E., 1996. The atmospheric winter circulation during the Younger Dryas stadial in the Atlantic/European sector. Climate Dynamics 12, 813–824.

Renssen, H., Isarin, R.F.B., Vandenberghe, J., Lautenschlager, M., Schlese, U., 2000. Permafrost as a critical factor in palaeoclimate modelling: the Younger Dryas case in Europe. Earth and Planetary Science Letters 176, 1–5.

Roeckner, E., Arpe, K., Bengtsson, L., Brinkop, S., Dümenil, L., Esch, M., Kirk, E., Lunkeit, F., Ponater, M., Rockel, B., Sausen, R., Schlese, U., Schubert, S., Windelband, M., 1992. Simulation of the present-day climate with the ECHAM model: impact of model physics and resolution. Report no. 93, Max Planck Institut für Meteorologie, Hamburg, 172pp.

Roeckner, E., Arpe, K., Bengtsson, L., Christoph, M., Claussen, M., Dümenil, L., Esch, M., Giorgetta, M., Schlese, U., Schulzweida, U., 1996. The atmospheric general circulation model ECHAM-4: model description and simulation of present-day climate. Report no. 218, Max-Planck-Institute für Meteorologie, Hamburg, 90pp.

Romanovskij, N.N., 1976. The scheme of correlation of polygonal wedge structures. Biuletyn Periglacjalny 26, 287–294.

Sarnthein, M., Jansen, E., Weinelt, M., Arnold, M., Duplessy, J.C., Erlenkeuser, H., Flatøy, A., Johannessen, G., Johannessen, T., Jung, S., Koc, N., Labeyrie, L., Maslin, M., Pflaumann, U., Schulz, H., 1995. Variations in Atlantic surface ocean paleoceanography, 50°–80°N: a time-slice record of the last 30,000 years. Paleoceanography 10, 1063–1094.

Sarnthein, M., Stattegger, K., Dreger, D., Erlenkeuser, H., Grootes, P., Haupt, B., Jung, S., Kiefer, T., Kuhnt, W., Pflaumann, U., Schäfer-Neth, C., Schulz, H., Schulz, M., Seidov, D., Simstich, J., van Krefeld, S., Vogelsang, E., Völker, A., Weinelt, M., 2000. Fundamental modes and abrupt changes in North Atlantic circulation and climate over the last 60 kyr—concepts, reconstruction, and numerical modelling. In: Schäfer, P., Ritzrau, W., Schlüter, M., Thiede, J. (Eds.), The Northern North Atlantic: A Changing Environment. Springer Verlag, Heidelberg.

Schiller, A., Mikolajewicz, U., Voss, R., 1997. The stability of the North Atlantic thermohaline circulation in a coupled ocean-atmosphere general circulation model. Climate Dynamics 13, 325–347.

Stocker, T.F., Wright, D.G., 1996. Rapid changes in ocean circulation and atmospheric radiocarbon. Paleoceanography 11, 773–795.

Stuiver, M., Reimer, P.J., Bard, E., Beck, J.W., Burr, G.S., Hughen, K.A., Kromer, B., McCormac, G., van der Plicht, J., Spurk, M., 1998. INTCAL98 radiocarbon age calibration, 24,000-0 cal BP. Radiocarbon 40, 1041–1084.

Vandenberghe, J., 1977. Geomorfologie van de Zuiderkempen. Verhandelingen Koninklijke Academie van Wetenschappen, Letteren en Schone Kunsten van België, Klasse der Wetenschappen 140, 160pp.

Vandenberghe, J., 1985a. Paleoenvironment and stratigraphy during the Last Glacial in the Belgian-Dutch border region. Quaternary Research 24, 23–38.

Vandenberghe, J., 1985b. Solution slots are ice-wedge casts? Mededelingen Rijks Geologische Dienst 39-1, 35–39.

Vandenberghe, J., 1988. Cryoturbations. In: Clark, M.J. (Ed.), Advances in Periglacial Geomorphology. John Wiley and Sons Ltd., Chichester, pp. 179–198.

Vandenberghe, J., Pissart, A., 1993. Permafrost changes in Europe during the Last Glacial. Permafrost and Periglacial Processes 4, 121–135.

Vandenberghe, J., Van de Broek, P., 1982. Weichselian convolution phenomena and processes in fine sediments. Boreas 11, 299–315.

Vandenberghe, J., Huizer, A.S, Mücher, H., Laan, W., 1998. Short climatic oscillations in a western European loess sequence (Kesselt, Belgium). Journal of Quaternary Science 13, 471–485.

Van den Haute, P., Van Craeynest, L., De Corte, F., 1998. The Late Pleistocene loess deposits and palaeosols of eastern Belgium: new TL age determinations. Journal of Quaternary Science 13, 487–497.

Van Huissteden, J., Vandenberghe, J., Van der Hammen, Th., Laan, W., 2000. Fluvial and eolian interaction under permafrost conditions: Weichselian Late Pleniglacial, Twente, eastern Netherlands. Catena 40, 307–321.

Van Vliet-Lanoë, B., 1992. Le niveau à langues de Kesselt, horizon repère de la stratigraphique du Weichselien supérieur Européen: signification paléoenvironmentale et paléoclimatique. Memoires Societé Géologique de France 160, 35–44.

Van Vliet-Lanoë, B., 1996. Relations entre la contraction thermique des sols en Europe du Nord-Ouest et la dynamique de l'inlandsis Weichsélien. Comptes Rendu Academie des Sciences de Paris 322 série IIa, 461–468.

Waelbroeck, C., Labeyrie, L., Michel, E., Duplessy, J.C., McManus, J.F., Lambeck, K., Balbon, E., Labracherie, M., 2002. Sea-level and deep water temperature changes derived from benthic foraminifera isotopic records. Quaternary Science Reviews 21, 295–305.